Wing Panel Design with Novel Skin-Buckling Containment Features

Wing Panel Design with Novel Skin Buckling Containment Features

G. Houston[1], D. Quinn[2] and A. Murphy[3]
Queen's University Belfast, Belfast, N. Ireland, BT9 5AH

and
F. Bron[4]
Constellium Technology Center, 38341 Voreppe, Cedex, France

The impact of Buckling Containment Features on the stability of thin gauge fuselage metallic stiffened panels has previously been demonstrated. With the continuing developments in manufacturing technology such as welding, extrusion, machining and additive layer manufacture, understanding the benefits of additional panel design features on heavier applications, such as wing panels, is timely. This compression testing of thick gauge panels with and without BCF has been undertaken to verify buckling and collapse behaviour and validate sizing methods. The experimental results demonstrate individual panel mass savings of the order of 9%, and wing cover design studies demonstrate mass savings of the order of 4 to 13%, dependent on aircraft size and material choice.

I. Introduction

To improve the stability and reduce the mass of metallic stiffened panels local skin bay Buckling Containment Features (BCF) have been proposed and experimentally demonstrated for thin gauge fuselage applications [1-4]. The introduction of panel skin bay BCF can increase the out-of-plane bending stiffness at the skin bay centre, significantly increasing the local initial buckling resistance, and resulting in increased performance typically accompanied with a reduction in the number of initial longitudinal buckle half-waves. Thus rather than buckling as a plate the panel skin bay will now buckle as a panel supported elastically on its edges by the larger lateral and longitudinal stiffeners. The

[1] Doctoral Research Student, School of Mechanical & Aerospace Engineering, Queen's University Belfast
[2] Lecturer, School of Mechanical & Aerospace Engineering, Queen's University Belfast
[3] Senior Lecturer, School of Mechanical & Aerospace Engineering, Queen's University Belfast
[4] R & D Engineer, Research Technology, Constellium Technology Center

available published experimental and computational analysis on the application of prismatic buckling containment features to thin gauge, low loaded, fuselage panels has suggested potential mass savings of the order of 15% [1]. Moreover the introduction of more design variables offers improved opportunity for local structural optimisation to local in-service loading [4]. This in turn will increase the potential to fully employ advances in manufacturing technology such as welding, extrusion, machining and additive layer manufacture, and new metallic material generations with improved stiffness, strength and durability properties. However to date no published data is available on the behaviour and potential benefits of additional panel design features on thick gauge panel applications such as those found in aircraft wing structures.

Thus this paper initially examines the static strength performance of integral metallic panels with an ultimate design load of 1500 N/mm. The experimental work focuses on two sets of compression test specimens, manufactured from aluminium-copper-lithium alloys and machined from thick plate, benchmarking the initial buckling and collapse performance of panel designs with and without BCF. The experimental results enable the validation of developed analytical structural sizing procedures to further understand the behaviour of BCF, considering a range of panel ultimate design loading. Based on the validated structural sizing procedure further analysis of the potential mass saving within idealised upper wing cover designs is evaluated, quantifying the benefits and defining the limitations of BCF to thick gauge panel applications.

II. Background

Significant percentage improvements in terms of panel weight and manufacturing cost, referenced to structural designs entering production now, are sought by the major airframe manufacturers for future aircraft. The combined targets constitute a significant challenge for both composite and metallic panel solutions. For metallic solutions the targets can potentially be best met through combined material, manufacture and design developments. In particular, the introduction of new manufacturing approaches have the potential to reduce manufacturing time and increase material buy-to-fly ratios, but additionally, they also enable the cost effective production of complex panel geometry. Herein near term manufacturing technologies are of interest, for example, high speed machining from near net shape plates or extrusions, built up via advanced welding processes [5-6]. Longer term enabling technologies may include wire based additive layer manufacture [7-8] or metal power deposition techniques [9]. To date the subtractive nature of machining from near net shape material introduces a low cost opportunity for local design features and published research has focused on using these design features to control panel local skin bay stability and durability:

Commented [DQ1]: References reordered sequentially as per Q4

Local panel design features introduced to control skin bay stability

The design of stiffened panels subjected to compression and shear loading during service must take into consideration the various buckling behaviours the panel may exhibit. For typical aircraft panel structures a number of buckling modes must be analysed, including buckling of the skin between the lateral and longitudinal stiffeners. Previous plate [10-12] and panel studies [13-16] have shown that local stability behaviour can be tailored by using non-uniform skin thicknesses. By further developing these principles it has been proposed that replacing the conventional uniform thickness skin bay with a reduced scale stiffened panel structure can potentially improve the structural efficiency of the skin element and provide additional design variables to enable improved local optimisation of the panel skin component [17]. As demonstrated by Quinn et al [1], the introduction of relatively small prismatic unflanged blade skin features within panel skin bays can significantly modify initial stability behaviour and improve both the initial buckling, and post buckling collapse performance. A series of initial experimental and computational studies on thin gauge structures, representative of typical low loaded, post-buckling aircraft fuselage components, demonstrates that by using additional skin features as panel Buckling Containment Features (BCF) panel initial buckling performance could be improved by up to 87.2%, and ultimate panel collapse performance improved by up to 17.7% [1]. The improvement in skin local stability is accomplished by designing the skin and additional skin features to initially buckle together as a combined unit between the typically larger primary longitudinal stiffeners and transverse rib or frame features. For these preceding studies, this modification of the skin local buckling behaviour is reflected by a reduction in the number of observed longitudinal buckle half-waves in the panel skin bays [1, 4, 18].

Commented [DQ2]: Corrected as per editing suggestion Q5

Furthermore, additional studies by Quinn et al [2] demonstrate that the introduction of non-prismatic, or off-axis orientated additional skin features can also effectively tailor panel local buckling behaviour and performance. Experimental and computational analyses, again on relatively low loaded, thin gauge panel structures exhibited improvements in both local buckling performance and ultimate panel collapse performance of a magnitude similar to those observed using prismatic blade additional skin features [2]. Additionally, to enable utilisation and application on typical aerospace stiffened panel components, Quinn et al [4] also proposed a method to enable initial static strength sizing of panels with additional skin features. The developed methodology relies on Finite Element analysis to generate bespoke skin buckling coefficients for simply supported plates with various skin and skin feature geometric combinations. The generated buckling coefficients are then used within traditional analytical buckling analysis methods in a manner that limits the modification to the conventional aerospace panel initial sizing process. To date,

the developed analytical sizing method has been validated solely for prismatic skin features within a low loaded, thin gauge stiffened panel design space.

Local panel design features introduced to control skin bay damage tolerance

In addition to panel buckling performance, fatigue and damage tolerance performance must also be considered when designing a stiffened panel if it is to be subject to cyclic loading during service. Similar to the potential to tailor buckling behaviour, it has been proposed that replacing the conventional uniform thickness panel skin bay with a non-uniform thickness or adding distributed design features can also improve the fatigue crack growth behaviour of aircraft stiffened panel components [19-22]. In experimental and numerical studies significant decrease in fatigue crack growth rates have been demonstrated [19, 21], considering both thick (wing) and thin (fuselage) skin thicknesses. The initial published results indicate that multiple regions of skin thickness variation, or crenellations, which are dimensionally wider than they are thicker, offer significant potential for improved panel life performance, with fatigue life gains of up to 100% observed [19]. Further experimental fatigue crack growth analysis on representative thin gauge fuselage stiffened panels demonstrated fatigue life gains of up to 63% when introducing prismatic blade skin features [3]. The introduction of these 'crack containment features' retard the growth of a crack by locally altering the stress intensity across the skin bay, whereby stress intensity reduces as the crack progresses into a containment feature and increases as the crack leaves the feature. Over the entire skin bay the net consequence of the local crack growth deceleration and acceleration through the skin features is a reduction of the global plate crack growth rate, and subsequent increase in fatigue life.

Whether the local skin bay features have been designed to control skin bay damage tolerance or stability, they have the potential to impact on panel buckling and collapse behaviour. However the relative scale of the local skin bay features to the gross panel dimensions will influence the impact level. To date experimental and computational studies focused on static strength have considered only thin gauge panel structure with relatively low ultimate design loads and low post-buckling ratios. Thus understanding and quantifying the sensitivity of thicker gauge panel design, with higher ultimate design loads and higher post-buckling ratios, to local skin bay features is a significant knowledge gap.

III. Experimental Validation

This section describes the experimental validation exercise whereby four sub-component specimens are manufactured and tested under compression loading for the purpose of validating developed analytical BCF analysis methods.

Test Specimen Design

A total of four specimens have been designed and manufactured for experimental test under compression loading. All specimens where designed for an ultimate collapse load of 1500 N/mm, representing the mean critical compression load on the upper wing cover of a single aisle aircraft. For all designs initial skin buckling and material yielding was not permitted to occur below specific load levels (87% of the ultimate load for buckling and 66% of the ultimate load for material yielding). These constraints match typical aerospace design requirements. The experimental specimens represent the minimum mass panel designs that simultaneously satisfy the ultimate collapse load, skin buckling load and material yielding requirements. For the four specimens the ultimate collapse load and the buckling constraint are the critical design drivers, whereas the yielding constraint is noncritical with the ultimate collapse load and skin buckling load requirements preventing material yielding below the specified limit. Two aluminium-copper-lithium alloys where used, an experimental high strength alloy (designated AL-HS) and a high damage tolerance alloy (AL-DT). Each material family includes a conventional panel and a panel containing Buckling Containment Features.

Figure 1 demonstrates the four specimens, where all specimens measure 1100mm in length, representing a full central rib bay and two outer half bays. Two representative rib features are attached to the panels for the purpose of replicating boundary conditions within the wingbox environment. Laterally, each specimen comprises three primary stringers with a fixed stringer pitch of 112.5mm and four skin bays. Specimen A is a conventional panel made from AL-DT with uniform thickness skin bays and prismatic T-section primary stringers. The rib features comprise a flat shear web fastened to integrated standing rib feet, as shown in Figure 1. Specimen B is an AL-DT panel with T-section primary stringers. There are two prismatic blade BCF in each skin bay, each of which measure 9mm in height (24% of primary stringer height) and 2.3mm in thickness (108% of skin thickness). As with Specimen A, the rib features comprise a flat web fastened to integral rib feet. The BCF are blended into the integral rib feet at each rib location. Specimen C is a conventional AL-HS panel with uniform thickness skin bays and T-section primary

stringers. The rib features represent a typical integral shear web and rib foot component fastened to the panel. To facilitate attachment to the panel via standard aerospace countersunk fasteners, the skin bays are locally thickened directly under the rib-panel joint locations. Specimen D is an AL-HS panel with T-section primary stringers. Again, the rib features represent typical rib shear web and foot geometry fastened to the panel in a manner identical to that of Specimen C. Two prismatic blade BCF are present in each skin bay, each measuring 10mm in height (31% of primary stringer height) and 2mm in thickness (100% of skin thickness). The BCF run the length of the panel continuously, passing through additional mouse holes located on the attached rib feet.

Table 1 Specimen designed and manufactured cross sectional areas (CSAs)

Test Specimen	Design CSA (mm^2)	Measured CSA (mm^2)	Panel Mass (kg)
Specimen A	2250	2273	6.94
Specimen B	1967	2028	6.21
Specimen C	2100	2118	6.48
Specimen D	1794	1876	5.76

Commented [DQ3]: Added as per suggestion Q8

Specimen Manufacture

Specimen panels and rib features are integrally machined separately from the aluminium alloy plate using a three axis milling machine and standard aerospace tooling and processes. Once manufactured the specimens are assembled using 6.35mm diameter titanium alloy Hi-Lite fasteners to attach the rib features to the stiffened panels. Once manufactured all specimen dimensions are measured to assess machining accuracy. The specimen plate sections, primary stringers and BCF were scanned for initial geometric imperfection patterns and each specimen accurately weighed. Table 1 details the manufactured specimen masses and cross sectional areas. All manufactured specimens are marginally heavier than designed. Examining both the global and local specimen machined geometry, the additional material corresponds to skin and BCF being thicker than designed. For the conventional panels, Specimen A and Specimen C, this increase in mass is +1.02% and +0.86% respectively. This additional mass is more evident on the BCF panels, where Specimen B and Specimen D are oversized by +3.1% and +4.6% respectively. Considering the equal target design load constraint that all specimens are subject to, the specimen range represents different design solutions, each of varying mass. Within the AL-DT family Specimen B is 10.5% lighter than Specimen A, and within the AL-HS family Specimen D is 11.1% lighter than Specimen C.

Figure 2 presents initial out-of-plane displacement imperfections measured on the skin side of each specimen using a Co-ordinate Measuring Machine. All specimens exhibit approximately similar geometric imperfections, with a single half wave curvature along the length of the specimen in the stiffener direction and a single half wave curvature across the width of the specimen. In all cases the direction of the curvatures are 'stiffener-out', that is to say the specimen panel imperfection is convex. Analysing the magnitude of the total curvature parallel to the primary stiffeners, the maximum out-of-plane imperfections are 0.16%, 0.27%, 0.26% and 0.34% of the specimen length for Specimens A, B, C and D respectively. Observation of the out-of-plane imperfection plots in Figure 2 indicates that these curvatures are most prevalent in the outer rib bays. When considering only the curvature in the key central test section between the attached rib features, the peak magnitudes are significantly lower; 0.06%, 0.06%, 0.03% and 0.07% of the specimen length for Specimens A, B, C and D respectively. The specimens with BCF exhibit higher imperfection curvatures than the conventional specimen. This may be attributed to the lower skin thicknesses and more intensive machining processes associated with the BCF designs.

Experimental Procedure

The specimens where tested in a load controlled 1500 kN capacity hydraulic testing machine. During test the rib features where restrained to prevent specimen out-of-plane displacement at the rib locations, while allowing the specimens freedom to end shorten, as shown in figure 3. Out-of-plane displacement along the panel longitudinal edges was also constrained within the test fixture to ensure that the outer skin bays behave as closed bays, also demonstrated in figure 3. A reinforced epoxy resin base (60 mm thick) was cast on to each specimen loading end. Once cast each specimen was marked and strain gauged in preparation for test. Strain gauges where located to assist in the determination of initial plate buckling and post-buckling collapse behaviour. Two calibrated displacement transducers, one either side of the specimen, were used to measure specimen end-shortening. To capture plate behaviour a three-dimensional Digital Image Correlation system was used (VIC-3D, Correlated Solutions) to measure skin out-of-plane displacement during the tests. The specimens were compression loaded in load control, at a rate of 5 kN/min until failure occurred.

Formatted: Not Highlight

Commented [DQ4]: Edited as per suggestion Q9

Experimental Results

Table 2 presents the experimentally measured initial plate buckling and ultimate panel collapse loads for Specimens A to D. For the determination of initial plate buckling, the parabolic strain differential method [23] was used with strain data from back-to-back gauges located at the same point on all specimens (the centre of the left hand central plate bay, as viewed from the panel un-stiffened side). Figure 4 presents the load versus end-shortening curves, illustrating specimen pre- and post-buckling stiffness. Figure 5 presents fringe plots of both specimen skin buckle modes captured from the Digital Image Correlation system. Figure 6 presents the specimen deformation mode as visually captured at the point of ultimate collapse.

Table 2 Comparison of experimental and analytically predicted failure and buckling performance

Test Specimen	Experimental Failure Load (kN)	Analytical Failure Load (kN)	Failure Load Variation	Experimental Buckling Load (kN)	Analytical Buckling Load (kN)	Buckling Load Variation
Specimen A	780.2	726.8	**-6.8%**	685	659	**-3.8%**
Specimen B	764.2	735.7	**-3.7%**	713	684	**-4.1%**
Specimen C	771.2	742.5	**-3.7%**	654	602	**-7.9%**
Specimen D	758.4	733.8	**-3.3%**	728	675	**-7.2%**

Specimen A

Specimen failure occurred at 780.2 kN by way of combined global stringer flexure (stringer out) and localised yielding of the stringer. Considering the number of effective skin-stringer units on the specimen to account for the influence of test boundary conditions and uneven distribution in the number of primary stringers and skin bays, the specimen failure load corresponds to a normalised panel loading intensity of 1646 N/mm. Initial skin buckling occurred at 685 kN, 88% of the specimens ultimate collapse load, with the central plate bays buckling anti-symmetrically into four longitudinal half-waves. This specimen exhibited a skin post-buckling mode change at 97% of the specimens ultimate collapse load, when five half-waves developed, more or less simultaneously, in each of the central bays.

Specimen B

Specimen failure occurred at 764.2 kN (1651 N/mm) by way of combined global stringer flexure (stringer out) and crippling of the stringer. Initial skin buckling occurred at 713 kN, 93% of the specimens ultimate collapse load,

with the central plate bays buckling anti-symmetrically into two longitudinal half-waves. The specimen maintained two skin buckle half waves through to panel failure.

Specimen C

Specimen failure occurred at 771.2 kN (1594 N/mm) by way of combined global stringer flexure (stringer in) and localised skin yielding. Initial skin buckling occurred at 654 kN, 85% of the specimens ultimate collapse load, with the central plate bays buckling anti-symmetrically into four longitudinal half-waves. The specimen maintained four skin buckle half waves through to panel failure.

Specimen D

Specimen failure occurred at 758.4 kN (1549 N/mm) by way of combined global stringer flexure (stringer in) and localised skin yielding. Initial skin buckling occurred at 728 kN, 96% of the specimens ultimate collapse load, with the central plate bays buckling anti-symmetrically into two longitudinal half-waves. The specimen maintained two skin buckle half waves through to panel failure.

Analysis of all four tests indicates that all specimens satisfy the ultimate load requirement (1500 N/mm), the initial buckling requirement (not below 87% of ultimate load) and the material yielding requirement (not below 66% of ultimate load). When considering ultimate loading intensities, the BCF panels matched the performance of their conventional counterparts, Specimen B collapsing within 0.3% of Specimen A (while being 10.5% lighter) and Specimen D collapsing within 0.3% of Specimen C (while being 11.1% lighter). At initial skin buckling both BCF panels initially buckled at higher loads that their conventional panel equivalent, Specimen B buckling +7.7% of Specimen A, and Specimen D buckling at +13.5% of Specimen C. The BCF panels demonstrated typical skin buckling behaviour, although with fewer longitudinal buckle half waves than the conventional panels. Additionally, the failure mechanisms of the BCF specimens are also consistent with those of their conventional equivalent designs. The only observed variation in specimen failure is that in addition to the localised skin yielding detected under the primary stringers on both conventional and BCF specimens, the BCF specimens also demonstrated localised skin yielding in the centre of the skin bays. These higher skin strain levels are a direct consequence of the significantly higher buckling loads of the BCF designs. Collectively, the series of experimental tests demonstrate that, when applied to thick gauge

wing type structures, the addition of BCF has the potential to offer more lightweight design solutions. Moreover, the initial buckling and ultimate collapse behaviour of thick gauge BCF panel structure is also consistent with that of traditional panel structures, and similar to that observed on thin fuselage gauge structures [1-2,18].

Analytical Analysis

Based on standard check stress techniques and procedures, a series of empirical and semi-empirical methods are employed to analyse the initial buckling and ultimate collapse performance of conventional stiffened panels under compression, tension and/or shear loading [24-27]. As detailed by Quinn et al [4], a tailored version of these analytical methods, adapted to facilitate skin BCF, can be used to analyse the initial buckling and ultimate failure performance of BCF panels. Table 2 presents the predicted initial skin buckling and ultimate failure loads of all specimens as analysed using these analytical methods. The experimentally measured material properties and measured dimensions after manufacture are used for the validation of the analytical analyses.

When compared to the experimental data, analytical analysis of Specimen A under predicts both initial skin buckling and ultimate collapse by 3.8% and 6.8% respectively. For Specimen B initial skin buckling and ultimate collapse predictions are conservative by 4.1% and 3.7% respectively. Initial buckling and ultimate collapse for Specimen C are again under predicted by 7.9% and 3.7% respectively. For Specimen D initial buckling and ultimate collapse are under predicted by 7.2% and 3.3% respectively.

Predictions of panel initial buckling and failure is consistently conservative, to an acceptable level of accuracy, for all specimens. The accuracy of BCF panel performance predictions (Specimen B and D) for both ultimate collapse and initial skin buckling is equivalent to that of the conventional panels (Specimen A and C). The developed analytical analysis methods may be considered validated for thick gauge panel structures, thus enabling additional design studies to further understand the full potential and/or limitations of BCF on more highly loaded, wing level aircraft structures.

IV. Panel Design Study

This section presents a study where single skin bay/stringer panels are sized both with, and without BCF to evaluate the sensitivity of mass savings to design loads, material properties and stringer pitch.

Panel Design Space

The design studies are performed using the validated analytical sizing methodology presented in [4]. The panel units designed comprise a single stringer and adjacent skin bays. All panels are optimised for minimum mass, subject to critical compression design load intensities ranging from 500 N/mm to 4000 N/mm. Panel units are also checked against non-critical tension (450-3600 N/mm) and shear (75-600 N/mm) loads representative of an upper wing cover load envelope. Local skin buckling is constrained not to occur below 87% of ultimate compression design load (equivalent to 130% limit load). Plastic material behaviour is also constrained not to occur below 66% of ultimate compression design load (equivalent to 100% limit load). For all design cases the panel length is fixed at 500mm, representative of typical wing rib pitch. Additionally, a minimum thickness constraint of 2mm is enforced on all panel thicknesses (skin, BCF and stringer elements) representative of current production limitations. Considering that the minimum stringer pitch on a tapered wing structure can vary based on manufacture and assembly requirements, the panel designs are optimised for two different minimum primary stringer pitch constraints: 100mm, typical of integral stiffened panel structures, and 125mm which is typical of built up riveted stiffened panel structures. To accommodate stiffened panels of varying primary stringer pitch the optimised panel mass is normalised, and presented, as cross sectional area per unit width.

Design Load and Stringer Pitch Sensitivity

Figure 7 presents the minimum mass designs for AL-DT T-stiffened panels, both with and without skin bay BCF, subject to a minimum stringer pitch constraint of 125mm. Comparing the optimal panel masses of conventional panel designs to those with skin BCF it is evident that for compression loading between 500 and 2500 N/mm the BCF designs are consistently lighter than conventional panel designs. Within this loading range, the relative weight savings of a BCF panel over a conventional panel is dependent on the magnitude of loading. Examining in detail individual designs, potential weight savings of greater than 15% are found between 100-1500 N/mm. As compression loading increases beyond this point the mass reductions associated with the introduction of skin BCF reduce. Similar behaviour is present when comparing conventional and BCF panel designs with a minimum stringer pitch of 100mm, Figure 8, where weight savings of greater than 10% are observed between 1000 and 1250 N/mm, with mass savings reducing as compression load increases beyond this point. Examining together Figure 7 and 8 it is evident that the weight savings of a BCF panel over a conventional panel is dependent on both the magnitude of loading and the

minimum primary stringer pitch. For compression loading intensities greater than 2750 N/mm the optimal panel masses are consistent, with minimal variation in weight associated with a change in primary stringer pitch or the introduction of skin BCF. For loading intensities in the range 500-2750 N/mm the optimal panel masses are sensitive to both primary stringer pitch and the presence of skin BCF. Within this range the conventional stiffened panels with a minimum stringer pitch of 100mm are consistently lighter than conventional panels with a minimum pitch of 125mm. These weight reductions are maximised at a compression loading of 1500 N/mm where the conventional 100mm stringer pitch panel is 12.2% lighter than the equivalent conventional panel with a stringer pitch of 125mm.

The varying sensitivity of BCF performance to load is associated with the variation in failure mechanisms. Inspection of the critical failure modes across the studied design space indicates that at higher levels of compression loading (>2000 N/mm) the panel designs are primarily driven by material yielding criteria. Stringer cross section crippling and combined yielding and flexure behaviour dominate the failure mechanisms. As compression loading decreases (<2000 N/mm) local skin instability criteria become increasingly prevalent in driving the panel designs. Thus the benefits associated with skin BCF are proportional to the relative influence of local stability failure criteria. For low to mid-level compression loading the local stability requirements are particularly critical and BCF technology can offer significant mass reductions.

Considering the sensitivity of the conventional panel mass to primary stringer pitch, the optimal panels with skin bay BCF appear relatively insensitive to the minimum primary stringer pitch constraint. Examining individual designs, for all conventional panel designs the optimally sized primary stringer pitch corresponds to that defined by the minimum pitch constraint. Driven by the requirement to satisfy local skin instability criteria the conventional panel designs tend towards the minimum primary stringer pitch allowed. Increasing the minimum stringer pitch directly translates into a thicker skin section, culminating in a heavier panel design. When considering the panel designs with skin BCF, however, an increase in minimum primary stringer pitch does not always require an increase in skin mass to satisfy the instability design criteria. The stability tailoring attributes of BCF technology allow the local instability design criteria to be satisfied through various combinations of equivalent mass skin bay geometries, incorporating either 100mm or 125mm primary stringer pitch options. As a consequence, the mass of optimal BCF panel designs with 100mm and 125mm minimum primary stringer constraints are relatively similar.

Table 3 Materials and associated properties used in the panel and wing cover design studies

Material	Modulus E_c (GPa)	Yield Stress σ_y (MPa)	Density (kg/m^3)
AL-DT	76.5	490	2700
AL-HS	78.3	590	2700
AL-7150	73.8	517	2823

Material Sensitivity

To evaluate the effect of material properties stiffened panels were also optimised using both the AL-DT and AL-HS materials, with a minimum primary stringer pitch of 125mm. Table 3 presents the key material mechanical properties and figure 9 presents the minimum mass designs. Figure 9 demonstrates that the relative impact of skin BCF on optimal panel mass is also sensitive to material properties, with the degree of sensitivity dependent on the particular design loads. When considering the conventional designs, the panel masses are relatively insensitive to the particular material selection to a load level of 1750 N/mm. Examining the BCF panel designs a similar pattern is found, with optimal panel mass insensitive up to a load level of 1250 N/mm. Considering individual designs, the maximum mass differences between the conventional and BCF panel designs are 17.6% and 18.4%, for AL-DT and AL-HS respectively. The compressive load intensity at which these maximum weight savings occur varies with the material, with the maximum mass difference occurring at 1000N/mm and 1750N/mm, with AL-DT and AL-HS respectively. Additionally, the choice of material also influences the point at which panels with skin BCF offer no weight reductions over conventional panels. The load at which the conventional and BCF panel masses are equivalent are 2500N/mm and 3250N/mm, with AL-DT and AL-HS respectively.

Again, inspection of the panel critical failure mechanisms across the investigated design space can explain the varying sensitivity of BCF effectiveness to material. At relatively low loading (<1250 N/mm) initial skin buckling and stringer flexural instability are the prominent critical failure mechanisms for both conventional and BCF panel designs. For highly loaded conditions (>3250 N/mm) all conventional and BCF panel designs are dominated by material limiting failure criteria such as stringer crippling and/or skin bay yielding. In the intermediate loading range (1250-3250N/mm) the sensitivity is dependent on when the critical failure mechanisms transition from stability criteria to material yielding criteria.

V. Wing Cover Case Study

The following section presents two case studies that assess how the weight reducing potential of BCF technology observed at individual panel level translates onto a global wing structure. Each case study uses the validated BCF design methodology [4] to size a complete upper wing cover. The wing cover sized in Case Study A is representative of a single aisle commercial aircraft wing and Case Study B sizes a wing cover representative of a smaller business jet aircraft. Figure 10 presents the compression loading distribution for Case Study A. The compression loads range from 1000N/mm to 4800N/mm, the accompanying shear loads range from 100N/mm to 500N/mm, and the tension loads range from 500N/mm to 3000N/mm. In Case Study B the compression loads range from 300N/mm to 2700N/mm, Figure 10, and the shear and tension loads range from 100N/mm to 400N/mm, and from 300N/mm to 2250N/mm respectively. The wing covers will be sized using AL-7150 T7751 (representing material technology employed in aircraft currently in production) and AL-HS (representing next generation material technology). The studies will create wing cover designs with and without skin BCF and with varying minimum stringer pitch constraints of 100mm and 125mm.

Case Study A: Commercial Aircraft Wing Cover

Table 4 presents the wing cover mass for the larger commercial wingbox (Case A), sized with various combinations of materials, BCF application and minimum primary stringer pitch. The sized wing cover masses range from 519.1kg (AL-7150 material, conventional skin bay and 125mm minimum stringer pitch) to 421.6kg (AL-HS material, with skin BCF and minimum stringer pitch of 100mm). When comparing the two material options, all AL-HS designs are consistently lighter than all AL-7150 designs. All designs using skin BCF technology are lighter than their equivalent conventional designs. Wing cover mass is also influenced by the minimum primary stringer pitch constraint. When directly comparing designs of equivalent material and skin BCF application, those with 100mm minimum stringer pitch constraint are consistently lighter than those with 125mm minimum pitch constraint.

Table 4 Summary of commercial wing cover mass, including mass difference between corresponding conventional (Conv.) and BCF designs.

Commented [DQ5]: Edited table as per suggestion Q12

	Minimum stringer pitch, mm					
	100			125		
	Conv. Skin configuration	BCF skin configuration	% difference	Conv. Skin configuration	BCF skin configuration	% difference

AL-7150 wing cover mass, kg	511.3	494.4	-3.3	519.1	503.2	-3.1
AL-HS wing cover mass, kg	430.5	421.6	-2.1	444.6	430.2	-3.2

Table 5 Summary of business jet wing cover mass, including mass difference between corresponding conventional (Conv.) and BCF designs.

	Minimum stringer pitch, mm					
	100			125		
	Conv. Skin configuration	BCF skin configuration	% difference	Conv. Skin configuration	BCF skin configuration	% difference
AL-7150 wing cover mass, kg	326.9	312.0	-4.6	337.2	314.8	-6.6
AL-HS wing cover mass, kg	267.3	249.1	-6.8	296.4	256.3	-13.5

Case Study B: Business Jet Wing Cover

Table 5 presents the wing cover mass for the smaller business jet wingbox (Case B). When comparing the two material options, all AL-HS designs are again consistently lighter than all AL-7150 designs. Weight savings offered by the AL-HS material option range from 12.1% (direct comparison of conventional designs with the 125mm minimum stringer pitch constraint) through to 20.2% (direct comparison of BCF skin bay designs with the 100mm minimum stringer pitch constraint). Again all BCF designs are lighter than their equivalent conventional designs. Similar to Case Study A, when directly comparing designs of equivalent material and skin BCF application, those with the 100mm minimum stringer pitch constraint are consistently lighter than those with the 125mm minimum pitch constraint.

Comparison of Wing Cover Applications

Formatted: Not Highlight

Formatted: Not Highlight

Commented [DQ6]: Edited table as per suggestion Q12

Formatted: Not Highlight

Formatted: Not Highlight

Formatted: Not Highlight

Studying both example wing cover applications, the application of skin bay BCF consistently offers potential weight saving benefits, where the magnitude of the mass savings are dependent on both material choice and primary stringer pitch constraints. For all combinations of materials and stringer pitch constraints, the mass reductions attributed to adding skin BCF over equivalent conventional skin designs is greater in Case Study B. Comparing equivalent designs with and without BCF technology, a maximum predicted weight saving of 13.5% is observed in Case B compared to a maximum weight saving of 3.3% observed in Case A. Considering the relationships identified on the local panel level study the difference between the two target wingbox applications appears directly related to the range and distribution of compression design loads on the respective wing covers. The panel level study indicates that the introduction of BCF technology is ineffective when compression loading exceeds a particular level (dependent on material and primary stringer pitch constraints).

Figure 11 presents the distribution of mass differences across the entire commercial upper wing cover for both the AL-7150 and AL-HS designs with the 125mm minimum primary stringer pitch constraint. Over the global wing cover there is a clear variation in localised predicted weight savings associated with the introduction of skin BCF. In the central region of the wing cover where compression loads are relatively high, the presence of skin BCF is relatively ineffective and offers minimal, if any, reduction in local panel mass. Towards the wing root and wing tip where compression loads are lower, the local predicted weight savings are significantly higher. On an individual panel level, local panel mass reductions of up to 17.8% on the AL-HS wing cover, and up to 17.6% on the AL-7150 wing cover are predicted. However, when combined with the apparent ineffectiveness of skin BCF technology in the higher loaded regions, the global averaged wing cover mass reduction is lower. In contrast, the distribution of lower loads on the Case B wing cover results in relatively high individual panel mass reductions predicted on all regions of the wing cover, culminating in a high total wing cover mass reduction observed when introducing skin BCF.

Commented [DQ7]: Edited as per suggestion Q13

Formatted: Not Highlight

Formatted: Not Highlight

Commented [DQ8]: Added to clarify figure description after figure caption was shortened – Q6

Formatted: Not Highlight

Formatted: Not Highlight

Formatted: Not Highlight

VI. Conclusions

Previous work has demonstrated the potential to introduce skin bay Buckling Containment Features to increase the local stability and static strength performance of thin gauge structural components such as aircraft fuselage panels. The work presented in this paper, for the first time demonstrates, through experimental and analytical analysis and

design, the potential of introducing Buckling Containment Features to improve the static strength performance, and thus reduce the weight, of thick gauge structural panel components such as those found on an aircraft wing box.

The experimental work focused on the sub-component level and examined the performance of thick gauge panels. To this end, four aluminium alloy specimens were designed, manufactured and tested to perform at an ultimate design load of 1500 N/mm. The experimental work demonstrates the potential of panels with BCF to match the performance of their equivalent conventional counterparts while being up to 11.1% lighter. Additionally, the experimental results validate the ability of previously developed analytical analysis methods to accurately predict the initial skin buckling and ultimate collapse performance of thick gauge panels with BCF.

Expanded panel analysis using the validated methodology highlights the sensitivity of BCF performance and weight saving effectiveness to both compression design loads and the material properties of the panel designs. The effectiveness of introducing BCF in reducing panel mass is maximised for compression loading between 1250 N/mm and 2000 N/mm, where local panel mass savings of up to 18.4% are possible. For compression loads greater than 2750 N/mm the introduction of skin BCF appears ineffective in reducing panel weight, with the transition of panel critical failure mechanisms from stability criteria to material yielding criteria being the limiting factor. BCF effectiveness is also predicted to improve by using higher performing materials, with the increased compressive stiffness and yield strength of advanced aluminium-copper-lithium alloys offering both greater magnitudes of mass savings and increasing the range of compression loads where BCF is effective.

Finally, two case studies evaluated the potential impact of introducing skin BCF technology on a global wingbox structure by sizing the upper wing covers of both a single aisle commercial aircraft and a business jet aircraft. The addition of skin BCF offers a potential global cover weight saving of up to 13.5% on the smaller business jet wing, and a weight saving of up to 3.3% on the larger single aisle wing. Variation in global wing impact appears dependent on the distribution of compression design loads on the respective wing covers, with the BCF appearing particularly ineffective on highly loaded regions of the single aisle wing cover, yet proving effective over the entire business jet wing cover.

Acknowledgments

The authors gratefully acknowledge the technical and financial support of Constellium Technology Center, Voreppe, France.

References

[1] Quinn, D., Murphy, A., McEwan,W., and Lemaitre, F., "Stiffened Panel Stability Behaviour and Performance Gains with Plate Prismatic Sub-Stiffening," *Thin-Walled Structures*, Vol. 47, No. 12, 2009, pp. 1457–1468. doi:10.1016/j.tws.2009.07.004

[2] Quinn, D., Murphy, A., McEwan,W., and Lemaitre, F., "Non-Prismatic Sub-Stiffening for Stiffened Panel Plates -Stability Behaviour and Performance Gains," *Thin-Walled Structures*, Vol. 48, No. 6, 2010, pp. 401–413. doi:10.1016/j.tws.2010.01.010

[3] Quinn, D., Murphy, A., and Cervi, L., "Fatigue Performance of Aircraft Panels with Novel Skin Buckling Containment Features," *Journal of Aerospace Engineering*, Vol. 225, July 2011, pp. 791–806. doi:10.1177/0954410011399035

[4] Quinn, D., Murphy, A., and Glazebrook, C., "Aerospace Stiffened Panel Initial Sizing with Novel Skin Sub-Stiffening Features," *International Journal of Structural Stability and Dynamics*, Vol. 12, No. 5, 2012, Paper 1250060. doi:10.1142/S0219455412500605

[5] Murphy, A., Ekmekyapar, T., Quinn, D., Özakça, M., Poston, K., Moore, G., and Niblock, J., "The Influence of Assembly Friction Stir Weld Location onWing Panel Static Strength," *Thin-Walled Structures*, Vol. 76, March 2014, pp. 56–64.
doi:10.1016/j.tws.2013.11.004

[6] McCune, R.W., Murphy,A. A., Price, M. M., and Butterfield, J. J., "The Influence of Friction Stir Welding Process Idealization on Residual Stress and Distortion Predictions for Future Airframe Assembly Simulations," *Journal of Manufacturing Science and Engineering*, Vol. 134, No. 3, 2012, Paper 031011.
doi:10.1115/1.4006554

[7] Mehnen, J., Ding, J., Lockett, H., and Kazanas, P., "Design for Wire and Arc Additive Layer Manufacture," *Proceedings of the 20th CIRP Design Conference*, edited by A. Bernard, Springer-Verlag Berlin Heidelberg, Germany, 2011, pp. 721-727.

Commented [DQ9]: Numbers reordered as per Q4

Commented [DQ10]: Updated with proceedings data – Q14

Formatted: Not Highlight

Formatted: Not Highlight

doi: 10.1007/978-3-642-15973-2_73

[8] Kazanas, P., Deherkar, P., Almeida, P., Lockett, H., and Williams, S., "Fabrication of Geometrical Features Using Wire and Arc Additive Manufacture," *Proceedings of the Institution of Mechanical Engineers, Part B: Journal of Engineering Manufacture*, Vol. 226, No. 6, 2012, pp. 1042–1051. doi:10.1177/0954405412437126

[9] Kapania, R., Design and Optimization of Structures Using Additive Manufacturing Processes, *ASM International 18th Advanced Aerospace Materials and Processes Conference and Exposition*, Paper MDI4.2, Aug. 2007.

[10] Petrisic, J., Kosel, F., and Bremec, B., "Buckling of Plates with Strengthenings," *Thin-Walled Structures*, Vol. 44, No. 3, 2006, pp. 334–343.
doi:10.1016/j.tws.2006.03.002

[11] Rahai, A. R., Alinia, M. M., and Kazemi, S., "Buckling Analysis of Stepped Plates Using Modified Buckling Mode Shapes," *Thin-Walled Structures*, Vol. 46, No. 5, 2008, pp. 484–493.
doi:10.1016/j.tws.2007.10.012

[12] York, C. B., "Buckling Interaction in Regular Arrays of Rigidly Supported Composite Laminated Plates with Orthogrid, Isogrid and Anisogrid Planform," *Journal of the American Helicopter Society*, Vol. 52, No. 4, 2007, pp. 343–359.
doi:10.4050/JAHS.52.343

[13] Bushnell, D., and Rankin, C., "Optimum Design of Stiffened Panels with Sub-Stiffeners," *46th AIAA/ASME/ASCE/AHS/ASC Structures, Structural Dynamics and Materials Conference*, AIAA Paper 2005-1932, April 2005.

[14] Watson, A., Featherston, C. A., and Kennedy, D., "Optimization of Postbuckled Stiffened Panels with Multiple Stiffener Sizes," *48th AIAA/ ASME/ASCE/AHS/ASC Structures, Structural Dynamics, and Materials Conference*, AIAA Paper 2007-2207, April 2007.

[15] Kapania, R., Li, J., and Kapoor, H., "Optimal Design of Unitized Panels with Curvilinear Stiffeners," AIAA *5th Aviation Technology, Integration and Operations Conference (ATIO)*, AIAA Paper 2005-7482, Sept. 2005.

Formatted: Not Highlight

Commented [DQ11]: Updated with organizer and paper ID – Q14

Formatted: Not Highlight

Formatted: Not Highlight

Formatted: Not Highlight

Formatted: Not Highlight

Commented [DQ12]: Updated with paper ID – Q14

Formatted: Not Highlight

Formatted: Not Highlight

[16] Ozakca, M., Murphy, A., and Van Der Veen, S., "Buckling and Post-Buckling of Sub-Stiffened or Locally Tailored Aluminium Panels," *ICAS 25th International Congress of the Aeronautical Sciences*, ICAS Paper 2006-10.4.3, Sept. 2006.

[17] Murphy, A., Quinn, D., Mawhinney, P., Ozakça, M., and van der Veen, S., "Tailoring Static Strength Performance of Metallic Stiffened Panels by Selective Local Sub-Stiffening," *47th AIAA/ASME/ASCE/AHS/ASC Structures, Structural Dynamics, and Materials Conference*, AIAA Paper 2006-1944, May 2006.

[18] Houston, G., Quinn, D., Murphy, A., Glazebrook, C., and Bron, F., "The Impact of Geometric Imperfections on Metallic Stiffened Panels with Skin Bay Buckling Containment Features," *53rd AIAA/ASME/ASCE/ AHS/ASC Structures, Structural Dynamics and Materials Conference*, AIAA Paper 2012-1960, April 2012.

[19] Muzzolini, R., and Ehrstrom, J. C., "Damage Tolerance of Integral Structures with Crack Retardation Features" *ASM International 15th Advanced Aerospace Materials and Processes Conference and Exposition,* Paper AFS3.6, June 2004.

[20] Lequeu, P., and Danielou, A., "Innovative High Performance Wing Concepts," *ASM International 17th Advanced Aerospace Materials and Processes Conference and Exposition (AeroMat 2006),* Paper ASLCM061.2, May 2006.

[21] Ehrström, J. C., Van der Veen, S., Arsène, S., and Muzzolini, R., "Improving Damage Tolerance of Integrally Machined Panels," *Proceedings of the 23rd Symposium of International Committee on Aeronautical Fatigue* , edited by C.D. Donne, German Society for Aeronautics and Astronautics (DGLR), Bonn, 2005, pp. 79-90.

[22] Bucci, R. J., "Advanced Metallic and Hybrid Structural Concepts: Tailorable Solutions to Meet the Demanding Performance/Affordability Requirements of Tomorrow's Aircraft," *ASIP Aircraft Structural Integrity Program Conference*, Nov. 2006.

[23] Singer, J., Arbocz, J., and Weller, T., *Buckling Experiments: Experimental Methods in Buckling of Thin-Walled Structures*, 1st ed., Wiley, New York, 1997, pp. 516-533

[24] Niu, M. C., *Airframe Structural Design*, 1st ed., Conmilit Press, Hong Kong, 1998.

Commented [DQ13]: Updated with paper ID – Q14
Formatted: Not Highlight
Formatted: Not Highlight
Formatted: Not Highlight
Formatted: Not Highlight
Commented [DQ14]: Updated with conference organizer and paper ID – Q14
Formatted: Not Highlight
Formatted: Not Highlight
Commented [DQ15]: Updated with conference organizer and paper ID – Q14
Formatted: Not Highlight
Commented [DQ16]: Updated with proceedings data – Q14
Formatted: Not Highlight
Formatted: Not Highlight
Formatted: Not Highlight
Commented [DQ17]: Updated with conference organizer – Q14
Formatted: Not Highlight
Formatted: Not Highlight
Commented [DQ18]: Updated with relevant page numbers – Q14
Formatted: Not Highlight

[25] Bruhn, E. F., *Analysis and Design of Flight Vehicle Structures*, 1st ed., Tri-State Offset Company, 1973.

[26] Timoshenko, S. P., and Gere, J. M., *Theory of Elastic Stability*, 2nd ed., McGraw–Hill Book Company, 1961.

[27] ESDU 70003., Local buckling of compression panels with unflanged integral stiffeners. *Engineering Sciences Data Units*, London, 1976, ISBN 978 1 86246 352 3

Commented [DQ19]: Updated with more detail – Q14

Formatted: Not Highlight

Formatted: Not Highlight

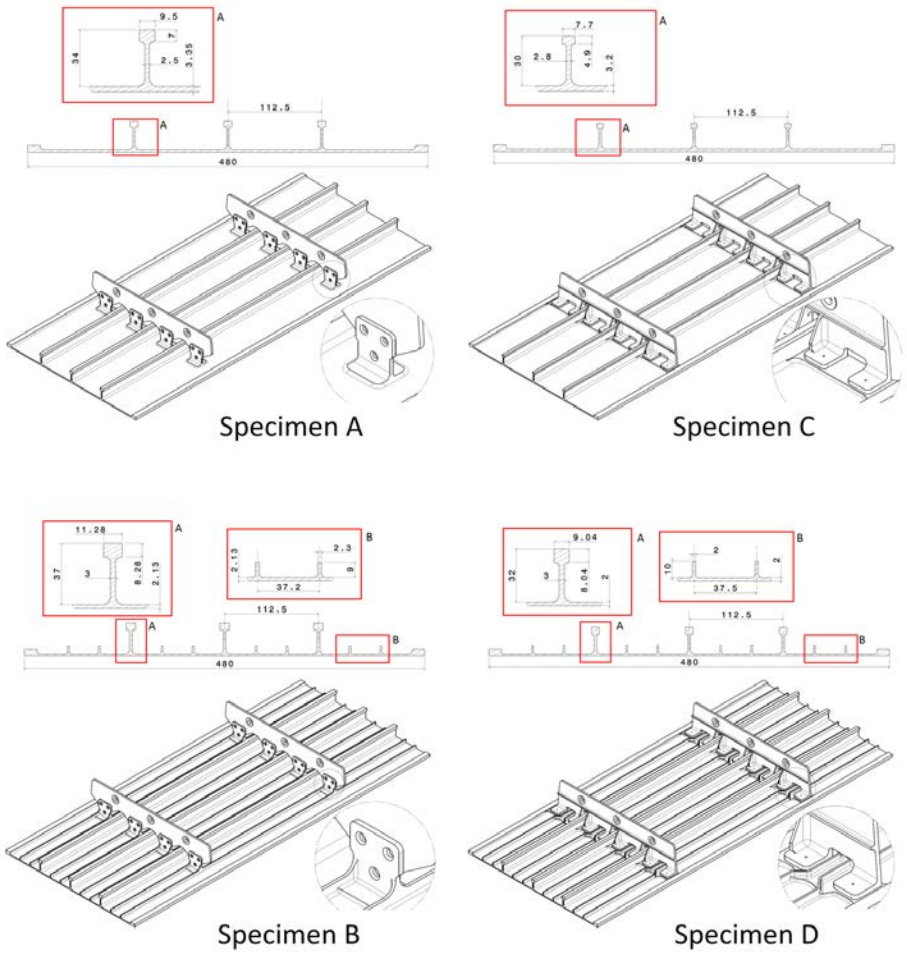

Fig. 1 Conventional and BCF wing cover panel specimens.

Commented [DQ20]: Edited to reduce caption length – Q6

Formatted: Not Highlight

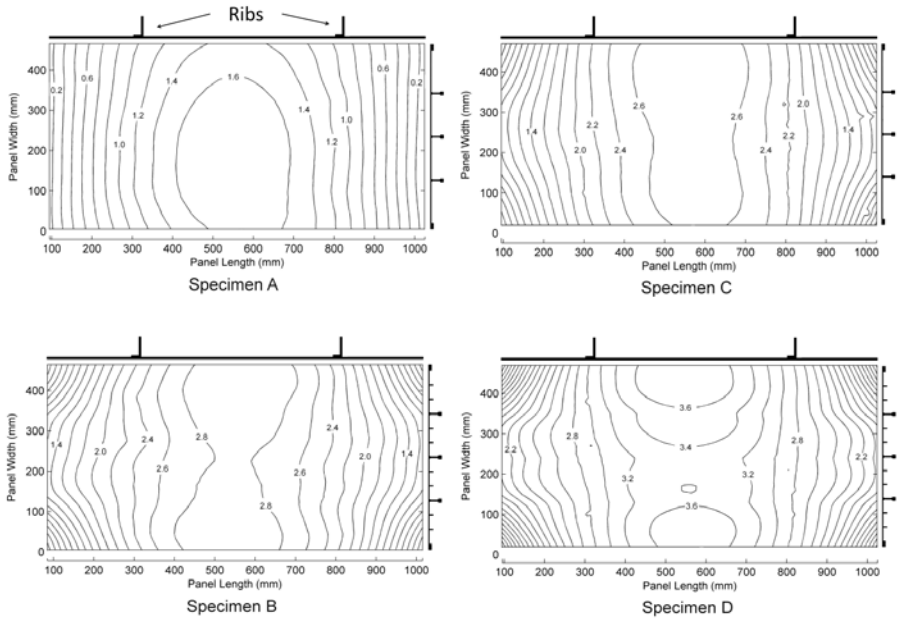

Fig. 2 Contours of initial specimen skin out-of-plane displacement.

Fig. 3 Specimen in test fixture as viewed from the stiffener side

Commented [DQ21]: Edited to reduce caption length – Q6

Formatted: Not Highlight

Formatted: Not Highlight

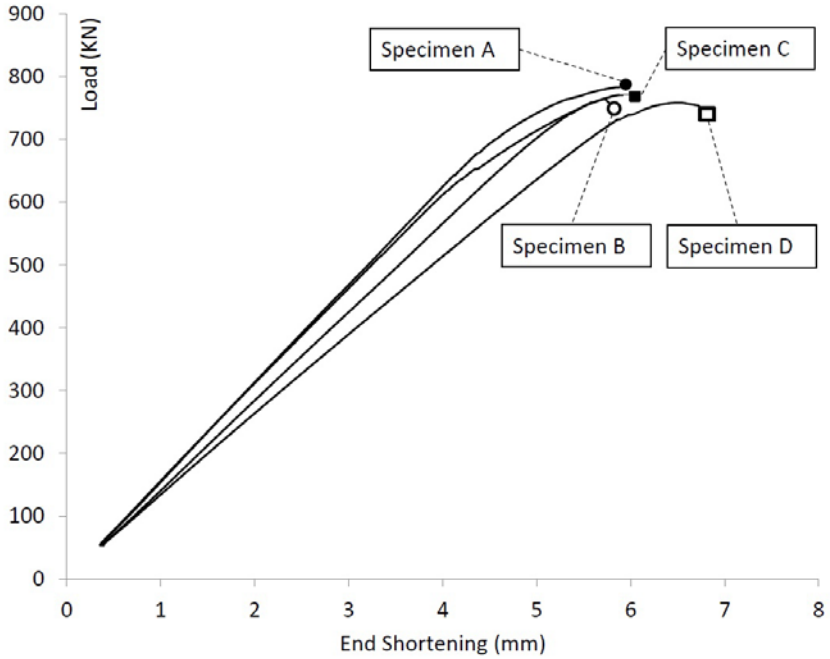

Fig. 4 Experimental load versus end-shortening curves for all four test specimens

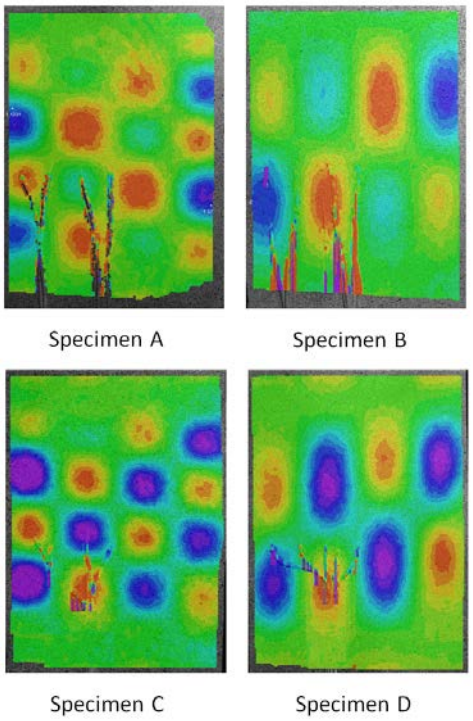

Fig. 5 Experimentally captured skin initial buckling mode forms

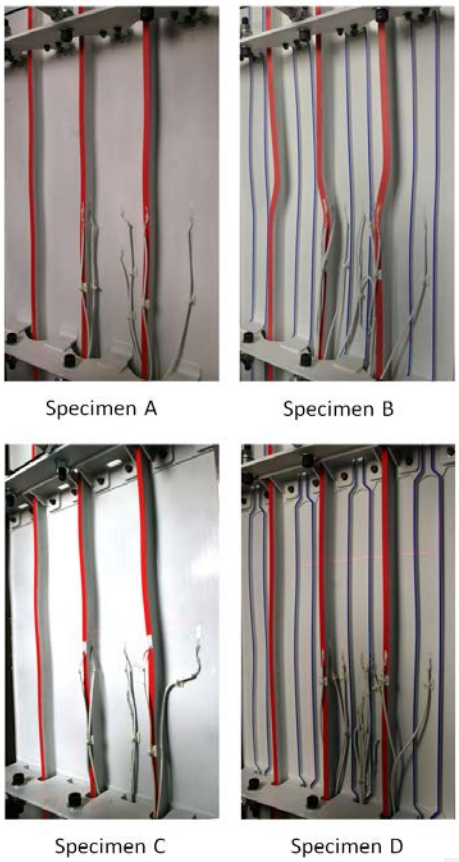

Fig. 6 Visual captures of experimental specimen ultimate failure mode

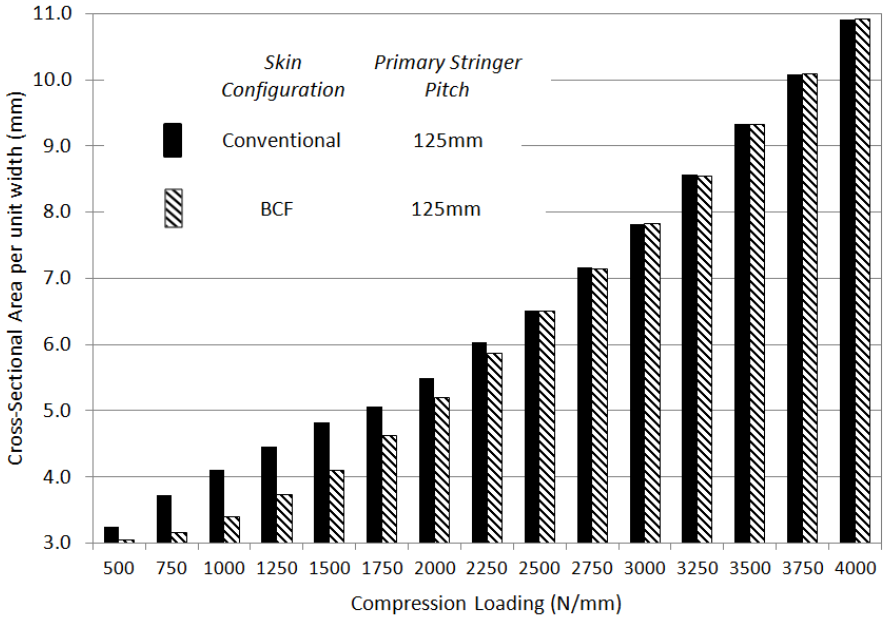

Fig. 7 Variation of optimised AL-DT panel mass (Cross-sectional area per unit width) with compression design loads.

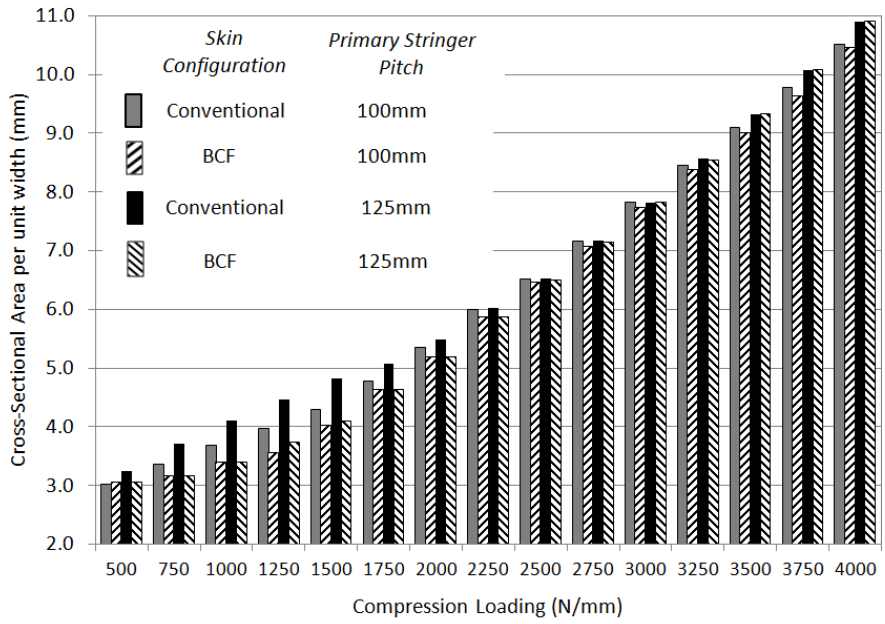

Fig. 8 Comparison of optimised conventional and BCF AL-DT panel mass (Cross-sectional area per unit width) for varying primary stringer pitch.

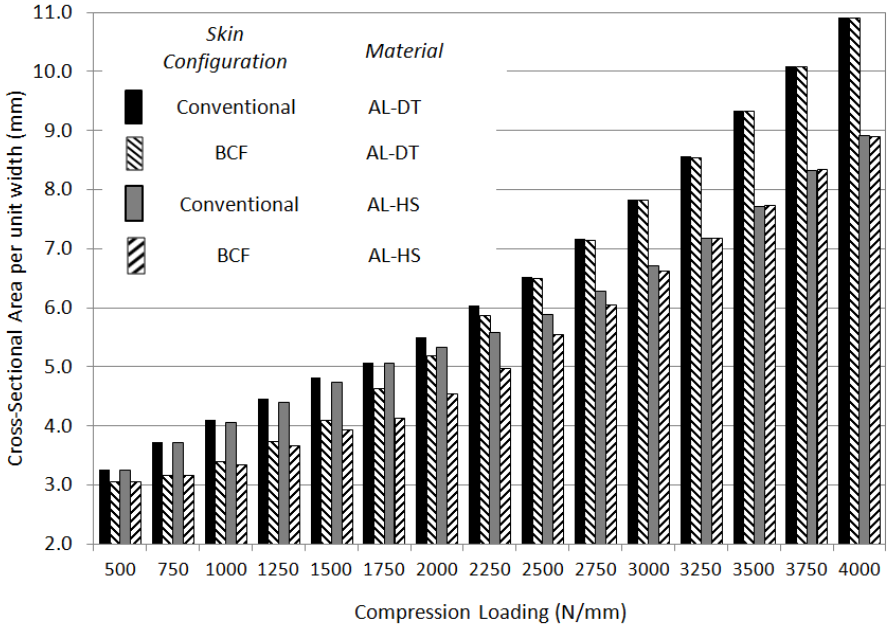

Fig.9 Comparison of AL-HS and AL-DT optimised panel mass (Cross-sectional area per unit width).

Commented [DQ22]: Edited to reduce caption length – Q6

Formatted: Not Highlight

Formatted: Not Highlight

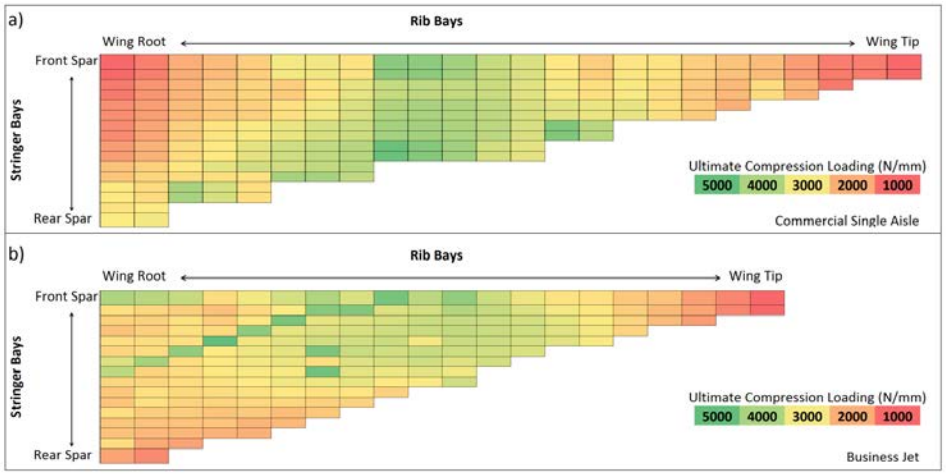

Fig. 10 Distribution of ultimate compression design loads for the commercial upper wing cover (a) and business jet upper wing cover (b) case studies.

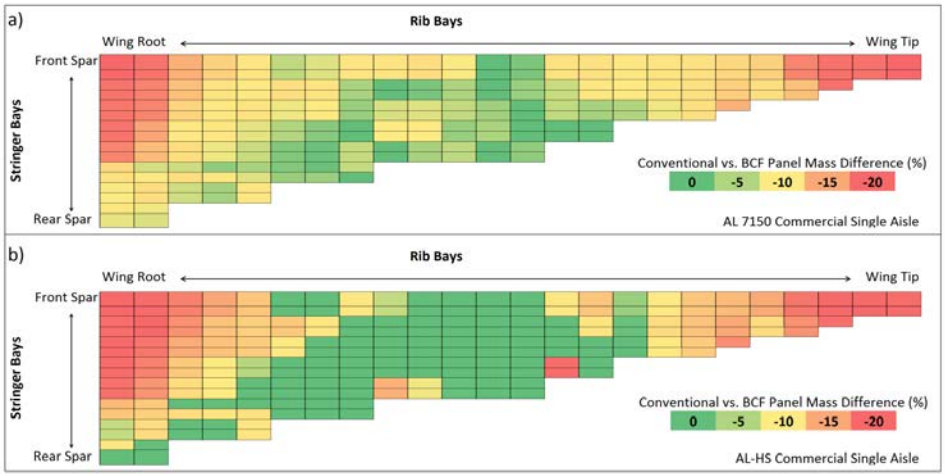

Fig. 11 Distribution of panel percentage weight savings for (a) AL-7150 and (b) AL-HS materials.

Commented [DQ23]: Edited to reduce caption length – Q6

Formatted: Not Highlight

Formatted: Not Highlight